

Mechanical and Optical Properties of Ion-exchange Strengthened Glass Coated with Sol-Gel Derived $\text{ZrO}_2\text{-SiO}_2$ Film

ZHANG He, ZHOU Jue-Hui, ZHANG Qi-Long, YANG Hui

(Department of Material Science and Engineering, Zhejiang University, Hangzhou 310027, China)

Abstract: $\text{ZrO}_2\text{-SiO}_2$ films of different SiO_2 content were deposited on soda-lime glass substrates through a Sol-Gel process, which was followed by an ion-exchange strengthening process. Phase presents, surface morphology and ion-exchange depth were determined by X-ray diffractometer, scanning electron microscope and energy dispersive spectrometer analysis, respectively. The mechanical and optical properties of coated glass were studied. Homogeneous, continuous and dense films are obtained. Pure ZrO_2 film belongs to tetragonal structure, while other films with SiO_2 have an amorphous structure. $\text{ZrO}_2\text{-SiO}_2$ films with high ratio ($H/E \geq 0.1$) and elastic recovery ($W_e \geq 60\%$) were thought to be favourable bending strength. Light transmittance increased, while hardness and Young's modulus decreased with the increasing SiO_2 content in films. Typically, chemical strengthened $0.5\text{ZrO}_2\text{-}0.5\text{SiO}_2$ film coated glass exhibited high bending strength of 393 MPa and high hardness of 18 GPa, and a negligible optical loss in visible region for thin thickness (~ 45 nm).

Key words: ion-exchange glass; Sol-Gel; $\text{ZrO}_2\text{-SiO}_2$ film; nanoindentation

Chemical strengthened soda-lime glass has been widely used in the window-shields of aircraft, high speed train cockpit and screen of digital products. However, because of the relatively low surface hardness, chemical strengthened soda-lime glass is susceptible to weakness from natural sands scratch^[1-4].

Certain improvements of mechanical resistance of the ion-exchanged glass substrate with Sol-Gel derived oxide film were reported^[5-15]. Especially, due to the high hardness, stiffness, strength and refractoriness, ZrO_2 system films were applied to enhance the scratch resistance of materials. At least two aspects of improvement were thought to be taken place when Sol-Gel ZrO_2 system films were applied to protect ion-exchanged glass surface. First, several investigations showed that the strength of glass was increased when covered by ZrO_2 or $\text{SiO}_2/\text{ZrO}_2$ Sol-Gel film^[8-10]. Second, glass exhibited a higher surface hardness value compared to that of original glass^[11-15]. However, light transmittance of glass dropped notably after coated with ZrO_2 film.

In the present work, $\text{SiO}_2\text{-ZrO}_2$ films with different SiO_2 contents were deposited on soda-lime glass substrates through a Sol-Gel process, which was followed by an ion-exchange strengthening process. The mechanical and optical properties of Sol-Gel derived films coated

glass were systematically studied.

1 Experimental Procedure

$\text{ZrO}_2\text{-SiO}_2$ films were prepared by Sol-Gel method using zirconium oxychloride, tetraethoxysilane (TEOS) and propylene epoxide with purities of over 99.9%. Stoichiometric amounts of zirconium oxychloride and tetraethoxysilane were dissolved in water-ethanol mixture. Propylene epoxide was added as gelling agent. After stirring was continued for 6 h at room temperature, the mixture turned into a transparent sol ($\text{pH} \approx 2.5$). Then, the coating was achieved by dipping glass substrates into the prepared sol and withdrawing at a constant speed of 60 mm/min using a dip-coating apparatus and consolidated at 60°C for 30 min. Coated glass samples were cured at 550°C for 2 h in air to obtain the solid films. The composition of soda-lime glass substrates is $74\text{SiO}_2\text{-}14\text{Na}_2\text{O-}11\text{CaO-}3\text{MgO-}1\text{Al}_2\text{O}_3\text{-}1\text{other}$ (in wt%), with the glass transition temperature (T_g) of $\sim 560^\circ\text{C}$. The molar compositions of $\text{SiO}_2\text{-ZrO}_2$ films were listed in Table 1. $\text{SiO}_2\text{-ZrO}_2$ films coated glass and uncoated blank sample glass were soaked in a melted potassium nitrate to induce $\text{Na}^+\text{-K}^+$ ion exchange at 450°C for 10 h.

Two different thick films (200 nm, 45 nm) were pre-

Received date: 2013-01-07; Modified date: 2013-02-18; Published online: 2013-03-28

Foundation items: National Key Technology Support Program (2009BAG12A07); Zhejiang Province Innovation Group Program (2011R09010)

Biography: ZHANG He(1983-), candidate of PhD. E-mail: crane507@qq.com

Corresponding author: YANG Hui, professor. E-mail: yanghui@zju.edu.cn

pared after heat treatment. Samples coated with ~ 200 nm ZrO_2 - SiO_2 films were used for nano-indentation test, samples coated with ~ 45 nm ZrO_2 - SiO_2 films were used for 3-point bending test, SEM and EDS measurement and both were used for transmittance spectra measurement. The aforementioned film thickness and refractive index were measured and identified by Elliptical polarization spectrograph (M-2000, J. A. Woollam, USA).

Continuous stiffness measurement (CSM) was applied as nanoindentation testing technique to study the hardness of films and glass surface on the nanoscale (Nano Indenter G200, Agilent, USA). The test was conducted under a constant nominal strain rate of 0.05 s^{-1} and frequency of 45 Hz. The harmonic displacement was 2 nm. A Poisson's ratio of 0.36 was used to calculate the Young's modulus. The measurements of average bending strength of specimens ($2 \text{ mm} \times 20 \text{ mm} \times 50 \text{ mm}$, grinded and polished the edges) were carried out with 3-point bending test (CMT5105, SANS, Shenzhen China). The reported mechanical property data correspond to an average value of 6 reliable tests. To characterize the optical properties, transmittance spectra were acquired at room temperature in the UV-V range ($\lambda = 250\text{--}800 \text{ nm}$) using a dual beam UV-3150 spectrophotometer (Shimadzu, Japan) with a step increment of 0.5 nm and an integration time of 0.3 s. Morphology and microstructure of the surface were characterized by scanning electron microscope (FESEM, S-4800, Hitachi, Japan). Ion-exchange depth was detected by Linear scanning in the direction of diffusion of potassium ion with energy dispersive X-ray spectrum (EDX, S-4800, Hitachi, Japan). Phase composition of films were determined by X-ray diffraction (XRD), employing a Shimadzu XRD-6000 diffractometer (Japan) with Bragg-Brentano geometry and $\text{Cu-K}\alpha$ radiation.

2 Results and discussion

2.1 Phase and surface morphology analysis

XRD patterns of ZrO_2 - SiO_2 films (~ 600 nm) with different SiO_2 contents are shown in Fig. 1. Pattern of pure ZrO_2 film (Zr100) is well indexed as a tetragonal structure. Patterns of other films with SiO_2 show no characteristic

diffraction peak, which indicates that these films have an amorphous structure. The representative SEM images of the Sol-Gel derived coating films (Zr100, Zr50 and Si100) are shown in Fig. 2. Homogeneous, continuous films are observed.

2.2 Mechanical properties

Hardness and Young's modulus were obtained by nano-indentation test. This test is especially applicable for thin solid film samples^[16]. The average hardness and Young's modulus of glass uncoated and coated with ZrO_2 - SiO_2 films are shown in Fig. 3. Values were measured from penetration depth at ~ 20 nm, which is about 0.1 of the thickness of films.

The nano-indentation hardness and Young's modulus of ZrO_2 - SiO_2 films (15–20 GPa, 145–185 GPa), ZrO_2 film (~ 22 GPa, ~ 190 GPa) are much higher than that of un-coated ion-exchanged glass (Blank, ~ 12 GPa, 120 GPa).

Table 1 Molar compositions of Sol-Gel derived ZrO_2 - SiO_2 composite films

Sample	Film thickness/nm	Composition/mol%	
		ZrO_2	SiO_2
Si100	$45 \pm 5/200 \pm 20$	–	100
Zr25	$45 \pm 5/200 \pm 20$	25	75
Zr50	$45 \pm 5/200 \pm 20$	50	50
Zr75	$45 \pm 5/200 \pm 20$	75	25
Zr100	$45 \pm 5/200 \pm 20$	100	–
Blank	–	–	–

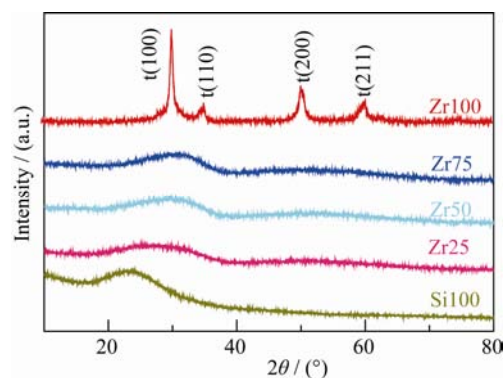


Fig. 1 XRD patterns for the films on glass substances after ion exchange process

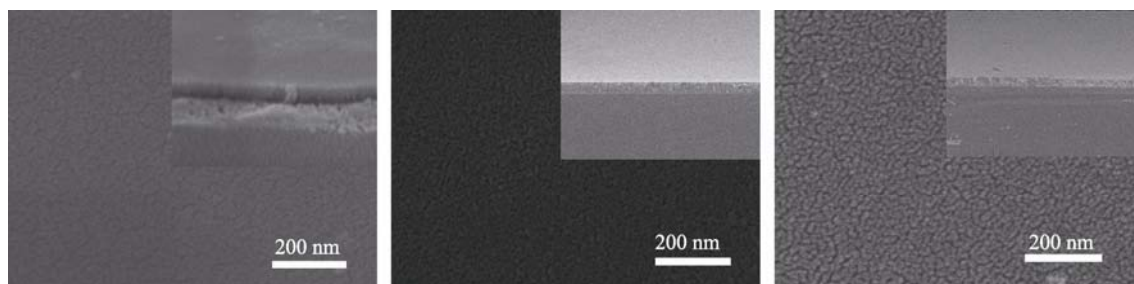


Fig. 2 SEM images of (a) ZrO_2 film, (b) ZrO_2 - SiO_2 composite film and (c) SiO_2 film surface and cross-section

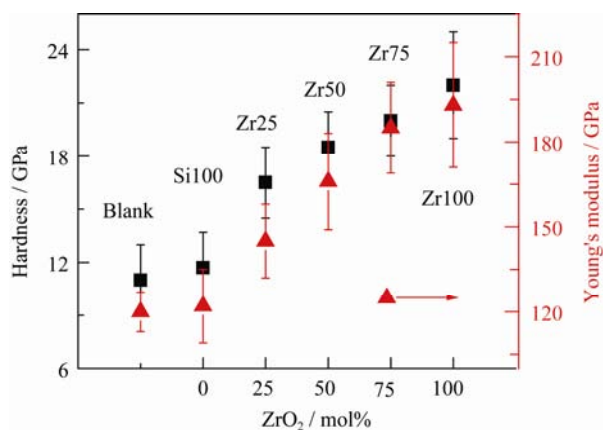


Fig. 3 Hardness and Young's modulus of glass coated with $\text{ZrO}_2\text{-SiO}_2$ films

As the composition of ZrO_2 in films increase, hardness and Young's modulus increase significantly, reaching up to twice that of un-coated ion-exchanged glass. These results indicate that the improvement in surface hardness and accordingly scratch resistance of ion-exchanged glass could be achieved by coating with Sol-Gel films.

Average values of 3-point bending strength, ion-exchange depth of coated and un-coated ion-exchanged glass, elastic recovery (W_e), hardness (H), Young's modulus (E) and (H/E) of films are presented in Table 2. The bending test was performed with thinner (45 nm) film, but there was no discernible difference in the strength of thicker (200 nm) samples. Ion-exchange depth is commonly believed to have positive impact to strength of glass, *i.e.*, strength increase with the increasing ion-exchange depth. However, in this study, glass coated with $\text{ZrO}_2\text{-SiO}_2$ films with smaller ion-exchange depth seems to shows similar 3-point bending strength with that of uncoated glass with greater ion-exchange depth (except for Zr100 sample). Complementary strength may be induced by coated films. Hard nanocomposite coatings with (i) a low value of the Young's modulus E satisfying high $H/E \geq 0.1$ ratio and (ii) a high value of the elastic recovery ($W_e \geq 60\%$) were thought to enhance strength^[17-18].

Weibull analysis was introduced to study the mechanism. Figure 4 shows the Weibull plots corresponding to

strength values of Blank and Si100 samples. The failure probability was calculated as

$$P_i = (i-0.5)/N \quad (1)$$

Weibull distribution equation:

$$\ln \ln[1/(1-P_i)] = m \ln \sigma_i + \ln[1/(\sigma_0)^m] \quad (2)$$

Where N is the total number of samples, we assign failure probability P_i to each value of σ_i after ranking all the 3-point bending test measured values in ascending order, i takes value from 1 to N which corresponds to the number of measurements of the sample tested; σ_i and σ_0 are failure strength and characteristic strength, respectively.

Equation (2) can be plotted as a straight line. In present work, $\ln \ln[1/(1-P_i)]$ versus $\ln \sigma_i$ whose slope is the Weibull modulus m by linear fitting the measured strength values^[19]. In Fig. 4, Si100 demonstrates a higher rupture resistance than uncoated glass according the distribution, however, the Weibull modulus m is less than that of uncoated glass. The result agrees with present coating strengthening theoretical model established by Carturan, *et al*^[10]. Strengthening effect of coating films promoted by crack length reduction and flaws healing are more pronounced for partial cracks of a smaller dimension than the average length, and that caused the Weibull modulus change^[19].

It is worth noting that the values of strength and ion-exchange depth increase with increasing SiO_2 content. The SiO_2 content in the films seemed to enhance the final

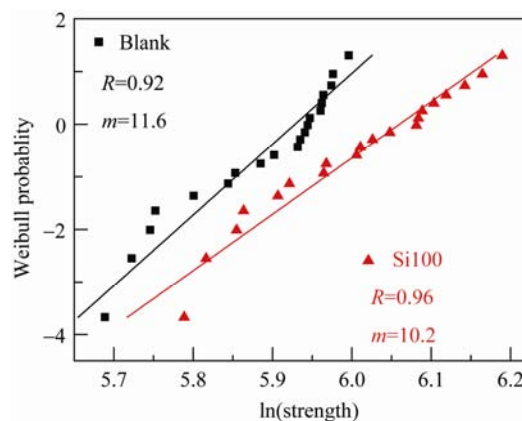


Fig. 4 Weibull plot of the Blank and Si100 samples after ion-exchange process

R : Correlation coefficient; m : Weibull modulus

Table 2 Three-point bending strength (MPa) and ion-exchange depth (μm) of $\text{ZrO}_2\text{-SiO}_2$ films coated glass

Sample	Zr100	Zr75	Zr50	Zr25	Si100	Blank
Average strength/MPa	350±37	370±36	393±39	401±40	409±37	361±27
Ion-exchange depth/ μm	15.9	16.2	16.7	17.0	17.2	17.6
Elastic recovery, $W_e/\%$	72.2	70	71	69.3	67	—
Film hardness, H/GPa	22	20	18.5	16.5	13.2	—
Young's modulus, E/GPa	193	185	166	145	122	—
H/E	0.114	0.108	0.111	0.113	0.108	—

glass strengthening effect. According to the previous investigation^[20], a possible explanation is proposed: zirconia is a well-known barrier material against alkali corrosion because of low alkali diffusion, while silica possesses much larger alkali diffusion coefficient. When silica content increases in the films, composite alkali ion diffusion coefficient would be improved. This could weaken the obstacle effect of films during ion-exchange process between glass surfaces and molten salt^[20-21].

2.3 Optical Properties

Figure 5 shows the transmittance spectra of un-coated and $\text{ZrO}_2\text{-SiO}_2$ films coated glass. Pure SiO_2 film coated glass shows a negligible optical loss, and Zr25, Zr50, Zr75 samples also show high transmittance reaching up to 85% at the wavelength of 350 nm and above. Pure ZrO_2 film coated glass exhibits lower transmittance compared to that of other samples. According to the XRD patterns shown in Fig. 1, Sol-Gel derived SiO_2 film and $\text{ZrO}_2\text{-SiO}_2$ films have amorphous structures, while pure ZrO_2 film shows a tetragonal structure. T-zirconia film performs greater optical scattering compared to that of amorphous film^[13,22], which could provide an explanation of the phenomenon described above. Figure 6 shows the refractive index versus wavelength of $\text{ZrO}_2\text{-SiO}_2$ films coated glass. Glass coated with more ZrO_2 content exhibit greater refractive index, which could cause more optical loss through reflec-

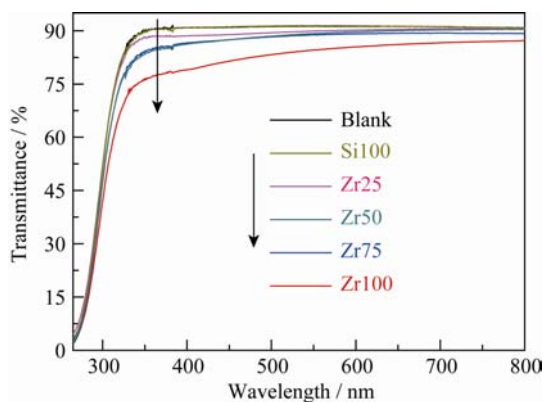


Fig. 5 Transmittance spectra of the samples after ion-exchange process

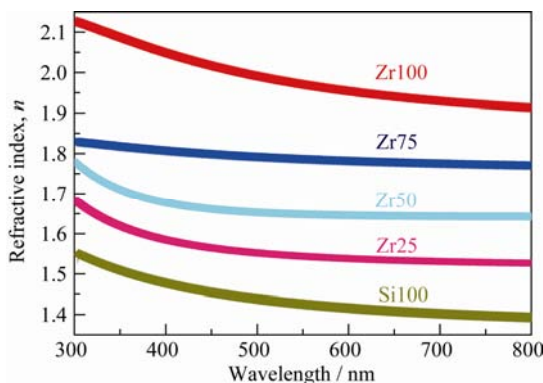


Fig. 6 Refractive index of the samples

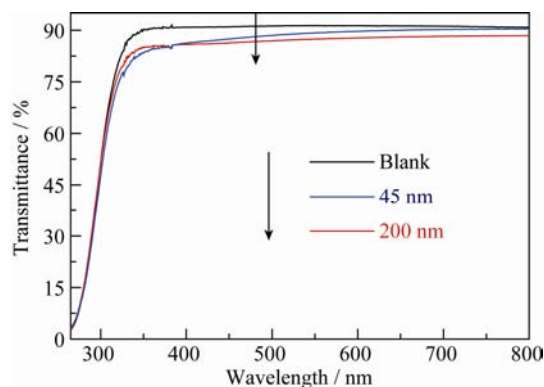


Fig. 7 Transmittance spectra of the samples (Zr50) with different film thickness

tion^[23-24]. This provides another aspect of the optical loss of pure ZrO_2 film coated glass. Moreover, notable decrease of transmittance could be found when increasing the coating thickness from 45 nm to 200 nm. More absorption loss would be happened in the thicker $\text{ZrO}_2\text{-SiO}_2$ film (typically: Zr50, shown in Fig. 7).

3 Conclusion

$\text{ZrO}_2\text{-SiO}_2$ films with different ZrO_2 contents were deposited on soda-lime glass substrates through a Sol-Gel process, which was followed by an ion-exchange strengthening process. $\text{ZrO}_2\text{-SiO}_2$ films with high $H/E \geq 0.1$ ratio and elastic recovery ($W_e \geq 60\%$) were thought to benefit bending strength. SiO_2 in the composition films could improve light transmittance while reduce the hardness and Young's modulus of films. However, the hardness could be improved by adding the ZrO_2 content. Typically, chemical-strengthened $0.5\text{ZrO}_2\text{-}0.5\text{SiO}_2$ film coated glass exhibited high bending strength of 393 MPa and high hardness of 18 GPa, but a negligible optical loss in visible region for very thin thickness (~45 nm).

References:

- [1] Nordberg Martin E, Mochel Ellen L, Garfinkel Harmon M, *et al.* Strengthening by ion exchange. *Journal of the American Ceramic Society*, 1964, **37**(5): 215–219.
- [2] Hale D K. Strengthening of silicate glasses by ion exchange. *Nature*, 1968, **217**: 1115–1118.
- [3] Bousbaa Chabane, Madjoubi Abderrahim, Hamidouche Mohamed, *et al.* Effect of annealing and chemical strengthening on soda lime glass erosion wear by sand blasting. *Journal of the European Ceramic Society*, 2003, **23**(2): 331–343.
- [4] Varshneya Arun K. Chemical strengthening of glass: lessons learned and yet to be learned. *International Journal of Applied Glass Science*, 2010, **1**(2): 131–142.
- [5] Sakka Sumio, Yoko Toshinobu. Sol-Gel-derived Coating Films and

- Applications. Chemistry, Spectroscopy and Applications of Sol-Gel Glasses, 1992: 89–118.
- [6] Uhlmann D R, Suratwala T, Davidson K, *et al*. Sol-Gel derived coatings on glass. *Journal of Non-Crystalline Solids*, 1997, **218**: 113–122.
- [7] Zheludkevich M L, Salvadob M, Ferreira M G S. Sol-Gel coatings for corrosion protection of metals. *Journal of Materials Chemistry*, 2005, **15**: 5099–5111.
- [8] Endres K, Mennig M, Amlung M *et al*. Enhancement of fracture strength of cutted plate glass by the application of SiO₂ Sol-Gel coatings. *Thin Solid Films*, 1999, **351(1/2)**: 132–136.
- [9] Fabes B D, Uhlmann D R. Strengthening of glass by Sol-Gel coatings. *Journal of American Ceramic Society*, 1990, **73(4)**: 978–988.
- [10] Carturan G, Khandelwal N, Sglavo V M, *et al*. Strengthening of soda-lime-silica glass by surface treatment with Sol-Gel silica. *Journal of Non-Crystalline Solids*, 2007, **353(16/17)**: 1540–1545.
- [11] Russak Michael A, Jahnes Christopher V, Katz Eric P, *et al*. Reactive magnetron sputtered zirconium oxide and zirconium silicon oxide thin films. *Journal of Vacuum Science and Technology*, 1989, **A7(3)**: 1248–1254.
- [12] Mehner A, Datchary W, Bleil N, *et al*. The influence of processing on crack formation, microstructure, density and hardness of Sol-Gel derived zirconia films. *Journal of Sol-Gel Science and Technology*, 2005, **36(1)**: 25–32.
- [13] Uhlmann Ina, Hawelka Dominik, Hildebrandt Erwin, *et al*. Structure and mechanical properties of silica doped zirconia thin films. *Thin Solid Films*, 2013, **527**: 200–204.
- [14] Watanabe Muneo. Chemical Method of Strengthening Glass Articles Subjected to Abrasion Resistance Treatment. US Patent, US4021218, 65/30 E, 1977.05.03.
- [15] Minosou Masao, Tonoike Masakiyo, Kawahara Hideo. Method of Manufacturing a Conductive Glass with High Strength and Wear Resistance. US Patent, US005279851A, 427/126.2, 1994.01.18.
- [16] Li Xiaodong, Bhushan Bharat. A review of nano-indentation continuous stiffness measurement technique and its applications. *Materials Characterization*, 2002, **48(1)**: 11–36.
- [17] Musil J. Hard nanocomposite coatings: thermal stability, oxidation resistance and toughness. *Surface & Coatings Technology*, 2012, **207**: 50–65.
- [18] Musil J, Kunc F, Zeman H, *et al*. Relationships between hardness, Young's modulus and elastic recovery in hard nanocomposite coatings. *Surface and Coatings Technology*, 2002, **154(2)**: 304–313.
- [19] Bergman B. On the estimation of the Weibull modulus. *Journal of Material Science Letters*, 1984, **3(8)**: 689–692.
- [20] Guglielmi Massimo. Sol-Gel coatings on metals. *Journal of Sol-Gel Science and Technology*, 1997, **8(1/2/3)**: 443–449.
- [21] Gy Rene. Ion exchange for glass strengthening. *Materials Science and Engineering B*, 2008, **149(2)**: 159–165.
- [22] Kuo D H, Chien C H, Huang C H. Zirconia and zirconia-silica thin films deposited by magnetron sputtering. *Thin Solid Films* 2002, **420-421**: 47–53.
- [23] Manifacier J C, Gasiot J, Fillard J P. A simple method of the determination of the optical constants n , k and the thickness of a weakly absorbing film. *Journal of physics E: Scientific Instruments*, 1976, **9(11)**: 1002–1004.
- [24] Feldman Albert, Ying Xuantong, Farabaugh E N. Optical properties of mixed yttria-silica films. *Applied Optics*, 1989, **28(24)**: 5229–5232.

ZrO₂-SiO₂ 薄膜对离子交换增强玻璃的光学和力学性能影响

张 鹤, 周珏辉, 张启龙, 杨 辉

(浙江大学 材料科学与工程学系, 杭州 310027)

摘 要: 采用溶胶-凝胶法在玻璃表面制备出 ZrO₂-SiO₂ 薄膜, 然后通过离子交换形成镀膜增强玻璃, 研究了薄膜组成对离子交换增强玻璃的力学和光学性能的影响。利用紫外可见分光光度计、激光椭圆仪、纳米压痕、三点抗弯和能谱(EDX)分析了薄膜结构及性能。结果表明: 所有薄膜均连续均匀, 纯 ZrO₂ 薄膜为四方相结构, 含 Si 薄膜为无定形结构; 薄膜具有较高弹性恢复率($\geq 60\%$)以及 H/E 比(≥ 0.1), 有利于强度增强; 随 Si 含量增加, 可见光透过率增大, 但表面硬度和杨氏模量随之降低; 0.5ZrO₂-0.5SiO₂ 薄膜综合性能最佳: 表面硬度为 18 GPa, 抗弯强度为 393 MPa, 厚度~45 nm 时可见光透过率大于 85%。

关 键 词: 离子交换玻璃; ZrO₂-SiO₂ 薄膜; 溶胶-凝胶; 纳米压痕

中图分类号: TQ174

文献标识码: A